RSC Advances

PAPER

View Article Online
View Journal | View Issue

Cite this: *RSC Adv.*, 2019, **9**, 11664

A ratiometric and colorimetric probe for detecting Hg^{2+} based on naphthalimide–rhodamine and its staining function in cell imaging †

Yuesong Wang, Haichang Ding, Shuai Wang, Congbin Fan, Yayi Tu, Gang Liu* and Shouzhi Pu*

Received 26th February 2019
Accepted 7th April 2019

DOI: 10.1039/c9ra01459d

rsc.li/rsc-advances

In this work, a rhodamine derivative was developed as a colorimetric and ratiometric fluorescent probe for Hg^{2+}. It exhibited a highly sensitive fluorescence response toward Hg^{2+}. Importantly, studies revealed that the probe could be used for ratiometric detection of Hg^{2+}, with a low detection limit of 0.679 μM. The mechanism of Hg^{2+} detection using compound **1** was confirmed by ESI-MS, ^1H NMR, and HPLC. Upon the addition of Hg^{2+}, the rhodamine receptor was induced to be in the ring-opening form *via* an Hg^{2+}-promoted hydrolysis of rhodamine hydrazide to rhodamine acid. In addition to Hg^{2+} detection, the naphthalimide–rhodamine compound was proven to be effective in cell imaging.

Introduction

Fluorescent probes have become powerful tools for the detection of heavy metal ions due to their low cost, high selectivity, and low concentration.[1–5] Among heavy metal ions, Hg^{2+} is one of the most troublesome ions because it easily goes through the biofilm, and then causes serious damage to the central nervous and endocrine systems.[6–10] In view of this, the synthesis of probes to identify Hg^{2+} has attracted sustained attention. So far, studies on Hg^{2+} probes have been mainly focused on using fluorescence intensity as an identifying signal.[11–15] However, these intensity-based probes have a range of disadvantages because intrinsic and extrinsic factors may affect the measurement of fluorescence intensity during the test.

Among fluorescent probes, the ratiometric fluorescent probe is designed to decrease the impact of these limitations.[16–20] Especially, probes based on fluorescent resonance energy transfer (FRET) have been increasingly studied.[21–23] FRET mechanism is interpreted as an interchange of energy between two excited fluorophore in which the donor power of excitation state is migrated to a non-radiative receptor unit. Well overlapped is superior to that of the sole fluorophore to achieve ratiometric change. This method demonstrates the ratiometric change in emission intensity of two different wavelengths, providing a synchronous recording of the ratio signal, which could provide self-modification of environmental impacts and afford an easy way to visualize complicated biologic procedures at the molecular level.[24–27] For example, Qian[28] *et al.* exploited a BODIPY–rhodamine probe for detecting Hg^{2+} on the ppb degree under physiological standards, which displays the non-interference and the same intensity of the emission bands. In order to validate the FRET process, the spectra of donor emission and acceptor absorption need to be well overlapped, which limits the layout and advancement of these probes. Therefore, it is imperative to construct a new ratiometric fluorescent probe to mitigate the limitations.

As a classic fluorophore, rhodamine-based fluorescent probes have been attracting increasing interests in the field of ion detection because of the high fluorescent quantum yield and long wavelength emission. Rhodamine materials are ideal candidates as energy receptors in the FRET system.[29–36] Besides rhodamine, naphthalimide is also a versatile fluorophore with easy manipulability, admirable stability and large stokes shift. The fluorescence emission of naphthalimide ranges from 470 nm to 570 nm, which overlaps with the absorption of rhodamine. It is promising to obtain ratiometric probe by connecting rhodamine and naphthalimide based on the FRET mechanism.

In this work, a fluorescent probe **1** with naphthalimide group as the energy donor and rhodamine as the energy acceptor was successfully designed and synthesized. The probe displayed a highly selective and sensitive detection for Hg^{2+} in CH_3CN–H_2O (7/3, v/v) solution.

Experimental

Materials and apparatus

4-Bromo-1,8-naphthalic, morpholine, 2-methoxyethanol, ethylenediamine, chloroacetyl chloride, trimethylamine, hydrazine

Jiangxi Key Laboratory of Organic Chemistry, Jiangxi Science and Technology Normal University, Nanchang, Jiangxi 330013, PR China. E-mail: liugang0926@163.com; pushouzhi@tsinghua.org.cn; Fax: +86-791-83831996; Tel: +86-791-83831996

† Electronic supplementary information (ESI) available. See DOI: 10.1039/c9ra01459d

monohydrate, benzotriazol-1-yloxytris(dimethylamino) phosphonium hexafluorophosphate, and anhydride were bought from Innochem (Beijing, China). The other reagents were purchased from J&K Chemicals. All reagents were analytical level and employed without further purification. Nitrate salts of metal ions (Cd^{2+}, Ni^{2+}, Co^{2+}, Ba^{2+}, Ca^{2+}, Pb^{2+}, Fe^{3+}, Cu^{2+}, Mg^{2+}, Mn^{2+}, Zn^{2+}, K^{+}, Sr^{2+}, Cr^{3+}, Al^{3+}, Ag^{+}) and the perchlorate salt of Hg^{2+} were used for appraising the combining capacity of ions to compounds. Deionized water was applied to the entire experiment.

^{1}H and ^{13}C NMR spectra were obtained on a Bruker AV400 NMR spectrometer using CD_2Cl_2 as the solvent and tetramethylsilane (TMS) as an internal reference. Mass spectrometry was conducted on an Agilent 1100 ion trap MSD spectrometer. HPLC spectra were taken on an Agilent 1260. An Agilent UV-8454 spectrophotometer was applied to the absorption measurements. The fluorescence spectra were collected using a Hitachi F-4500 fluorescence spectrophotometer. The melting points were determined by a WRS-1B melting point apparatus. The staining of cells was performed using an OLYMPUS FV1000 confocal laser scanning microscope. The fluorescence quantum yield value was recorded by a machine named QY C11347-11.

Methods

A mixture of **1** (1.0×10^{-3} mol L^{-1}) was ready in 2.0 mL CH_3CN–H_2O (7/3, v/v) solution, which was used for the fluorescence and absorption studies with proper concentration of metal ions at room temperature. The detection experiments of metal ions were gained by adding 5.0 eq. metal ions into 2.0 mL CH_3CN–H_2O (7/3, v/v) solution of **1** (2.0×10^{-5} mol L^{-1}). The excitation and emission slit of fluorescence measurements were carried out with 5 nm and 10 nm ($\lambda_{ex} = 410$ nm).

Synthesis

The synthetic route for **1** was shown in Scheme 1. Compound **2** was obtained from commercial suppliers, and compound **3**, **4**, **5** and **6** were synthesized by the composited methods.[37,38]

Synthesis of 7. A stirred solution of compound **5** (0.60 g, 1.50 mmol), compound **6** (0.68 g, 1.50 mmol) and NaH (0.07 g, 3.00 mmol) in anhydrous CH_3CN (30 mL) was refluxed for 8 h under argon atmosphere. Then the reactive solution was cooled to room temperature and quenched with ice water. The mixture was extracted with dichloromethane, desiccated over Na_2SO_4. The crude product was evaporated and scavenged by column chromatography using CH_2Cl_2/C_2H_5OH (30 : 1, v/v) as eluent, and then gained compound **7** (0.48 g, 0.60 mmol) as red solid in 38%. Mp 447–449 K; ^{1}H NMR (400 Hz, CD_2Cl_2), δ (ppm): 8.54 (d, $J = 8.0$ Hz, 1H), 8.45 (t, $J = 6.0$ Hz, 2H), 7.99 (d, $J = 8.0$ Hz, 1H), 7.70 (t, $J = 8.0$ Hz, 2H), 7.64 (d, $J = 8.0$ Hz, 1H), 7.60 (d, $J = 8.0$ Hz, 1H), 7.19 (d, $J = 8.0$ Hz, 2H), 6.63 (t, $J = 8.0$ Hz, 2H), 6.55 (t, $J = 10.0$ Hz, 2H), 6.47 (s, 1H), 6.38 (d, $J = 8.0$ Hz, 1H), 4.37 (t, $J = 4.0$ Hz, 2H), 3.94 (s, 4H), 3.65–3.63 (m, 2H), 3.41–3.36 (m, 4H), 3.21 (d, $J = 16.0$ Hz, 8H), 2.93 (s, 2H), 2.58 (s, 4H), 1.18 (t, $J = 8.0$ Hz, 6H) (Fig. S1†); ^{13}C NMR (100 MHz, CD_2Cl_2), δ (ppm): 169.32, 168.60, 163.93, 163.48, 155.36, 152.47, 152.13, 149.10, 133.87, 131.87, 130.36, 129.75, 129.26, 128.67, 128.06, 127.84, 126.89, 125.49, 125.07, 123.99, 123.29, 122.35, 115.85, 114.22, 110.62, 109.11, 107.73, 104.99, 101.02, 96.84, 66.10, 60.60, 47.45, 43.76, 38.45, 37.51, 28.93, 11.55 (Fig. S2†); ESI-MS (m/z): 821.2 ($[\mathbf{M_7}]^{+}$), calculated for $C_{48}H_{49}N_6O_7$: 821.3 (Fig. S3†).

Synthesis of 1. Compound **7** (0.12 g, 0.15 mmol) and hydrazine monohydrate (0.03 g, 0.60 mol) were added to CH_2Cl_2 (20 mL) with BOP (0.01 g, 0.03 mmol) under argon atmosphere. After stirring for 2 h, the crude product was purified by column chromatography on silica gel using CH_2Cl_2/C_2H_5OH (40 : 1, v/v) as the eluent, and then obtained target compound **1** (0.12 g, 0.14 mmol) as yellow solid in 93% yield. Mp 456–458 K; ^{1}H NMR (400 MHz, CD_2Cl_2), δ (ppm): 8.55 (d, $J = 8.0$ Hz, 1H), 8.48 (d, $J = 8.0$ Hz, 1H), 8.45 (d, $J = 8.0$ Hz, 1H), 7.87–7.89 (m, 1H), 7.71 (t, $J = 8.0$ Hz, 1H), 7.56 (s, 1H), 7.50–7.48 (m, 2H), 7.23 (d, $J = 8.0$ Hz, 1H), 7.07–7.05 (m, 1H), 6.64 (s, 1H), 6.53 (d, $J = 8.0$ Hz, 1H), 6.51 (d, $J = 4.0$ Hz, 1H), 6.47 (s, 1H), 6.45 (s, 1H), 6.34 (d, $J = 8.0$ Hz, 1H), 4.38 (t, $J = 6.0$ Hz, 2H), 3.95 (t, $J = 4.0$ Hz, 4H), 3.71 (s, 2H), 3.67–3.62 (m, 2H), 3.39–3.34 (m, 4H), 3.24 (t, $J = 4.0$ Hz, 4H), 3.18 (s, 4H), 2.94 (s, 2H), 2.59 (s, 4H), 1.17 (t, $J = 6.0$ Hz, 6H) (Fig. S4†); ^{13}C NMR (100 MHz, CD_2Cl_2), δ (ppm): 169.38, 165.15, 163.91, 163.44, 155.33, 152.90, 152.73, 151.45, 150.93, 148.33, 131.81, 131.71, 130.35, 129.71, 127.51, 127.18, 125.07, 122.82, 122.04, 115.95, 114.24, 110.73, 108.60, 107.60, 104.10, 101.57, 97.25, 66.12, 64.64, 60.65, 47.60, 43.65, 38.45, 37.44, 11.60 (Fig. S5†); ESI-MS (m/z): 835.2 ($[\mathbf{M_1} + H^{+}]^{+}$), calculated for $C_{48}H_{50}N_8O_6$: 834.3 (Fig. S6†).

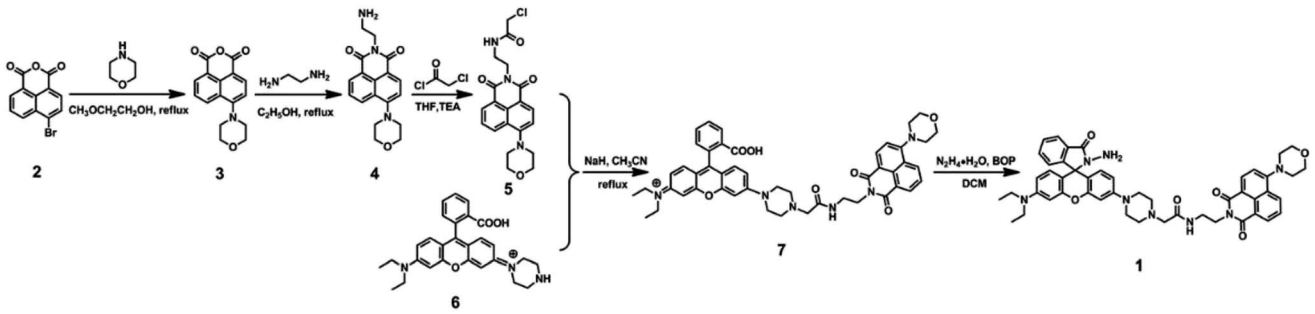

Scheme 1 Structure and synthesis of **1**.

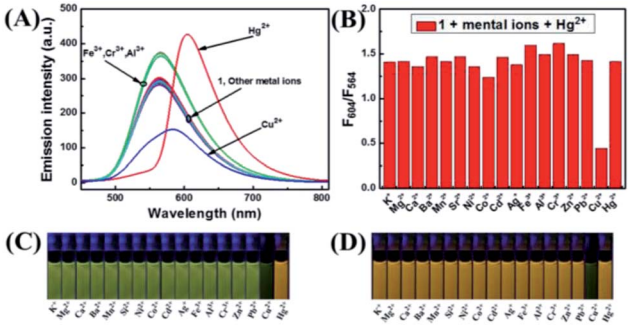

Fig. 1 Mutations in the fluorescence spectra of **1** induced by the ions mentioned above in the CH_3CN–H_2O (7/3, v/v) solution: (A) fluorescent spectral changes; (B) emission intensity alterations; (C) the change of fluorescence color induced by various ions; (D) the change of fluorescence color of **1** upon addition of 5.0 eq. Hg^{2+} in the existence of 5.0 eq. interfering ions.

Results and discussion

Fluorescence spectral responses of probe 1 to metal ions

The selectivity of **1** was investigated by fluorescence spectroscopy. Fig. 1A showed the emission spectra of **1** (20 μM) in CH_3CN–H_2O (7/3, v/v) solution while being excited at 410 nm. Probe **1** showed an emission peak at 564 nm, which was ascribed to the fluorescence of the naphthalimide group. As shown in Fig. 2, by adding Hg^{2+}, the characteristic fluorescence of rhodamine at 604 nm emerged quickly and the peak at 564 nm decreased gradually with an apparent color change from green to orange. The accession of Hg^{2+} triggered the ring-opening of the spirolactam of the rhodamine part that was useful for the acquisition of fluorescence resonance energy from the naphthalimide portion. Among these metal ions, some ions (Fe^{3+}, Al^{3+}, Cr^{3+}) only induced single-signal slight fluorescence enhancement and Cu^{2+} could slightly quench the fluorescence. Subsequently, in order to evaluate the anti-interference ability of **1** for detecting Hg^{2+}, a series of experimentations were conducted to observe the ratio variation in the fluorescence strength between 604 nm and 564 nm with the addition of 5.0 eq. of Hg^{2+} to the mixture of **1** in the existence of other metal ions (5.0 eq.). As shown in Fig. 1B, the result suggested that metal ions other than Cu^{2+} had no influence on the Hg^{2+}-induced fluorescence responses.

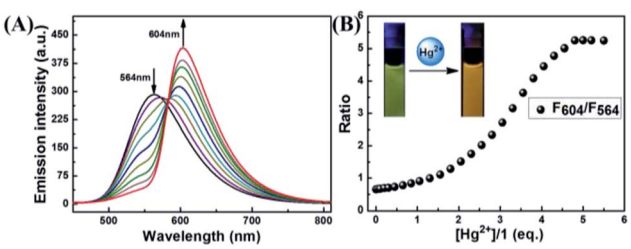

Fig. 2 (A) The fluorescence variation of **1** induced by Hg^{2+}; (B) the curve of fluorescent intensity ratio at 564 nm and 604 nm with the addition of different eq. of Hg^{2+}.

The fluorescence spectra of probe **1** treated with a range of concentrations of Hg^{2+} in CH_3CN–H_2O (7/3, v/v) solution were recorded with results shown in Fig. 2A. The spectra of **1** exhibited fluorescence emission at 564 nm of naphthalimide section and no obvious emission at 604 nm of rhodamine group was detected. Adding Hg^{2+} (0–5.0 eq.) to the CH_3CN–H_2O (7/3, v/v) solution of **1**, the strength of the naphthalimide peak decreased, while a new peak belonged to the characteristic peak of rhodamine appeared and gradually increased, indicating the FRET process had occurred. When the concentration of Hg^{2+} was added to 5.0 eq., the ratio of emission intensities (F_{604}/F_{564}) remained unchanged and the fluorescent color of the solution of probe **1** transformed from green to orange. The quantum yield of fluorescence for probe **1** was calculated as $\Phi = 0.410$ (for $\lambda_{em} = 564$ nm), whereas the worth of **1**–Hg^{2+} complex belonged to 0.029 (for $\lambda_{em} = 604$ nm). In the concentration ranging from 0 to 21 μM, the variation of ratio of emission intensities (F_{604}/F_{564}) revealed a fine linear relationship ($Y = 2.33097X + 188.4710$, $R = 0.994$) with the concentration of Hg^{2+} (Fig. S7A†). The detection limit was calculated to be 2.334 μM based on $3\sigma/k$ (Fig. S7B†) (σ stands for the standard deviation of the blank signal and k indicates the ratio of grade for the linear calibration plot).[39,40] The present probe was compared with other probes reported for Hg^{2+} detection in recent years,[7–10] As shown in Table 1, these results revealed that probe **1** could detect a low level of Hg^{2+}. These probes showed some good physical properties such as linear range, lower LOD, high sensitivity and so on. For the **1** + Hg^{2+} complex, a moderate performance in all aspects was observed, suggesting that probe **1** could serve as a fluorescence probe for Hg^{2+}.

Absorption responses of 1 to metal ions

According to Fig. 3A, the absorbance of probe **1** showed only the characteristic absorption peak of the donor (naphthalimide) at 401 nm. The addition of 5.0 eq. Hg^{2+} instantly led to a remarkable increase in the absorption of rhodamine at 554 nm, and the color of the solution changed from light yellow to pink as observed by naked eyes. When 5.0 eq. of Cu^{2+} was added in the solution, the absorbance was markedly increased with a new peak arising at 697 nm. Next, we carried out competitive trials for the anti-interference capability of **1** + Hg^{2+}. As shown in Fig. 3B, although the absorption of Cu^{2+} had a notable red shift, it was perfectly staggered and had no interference with the absorption peak at 554 nm. In titration experiments with Hg^{2+}, absorption spectra of **1** + Hg^{2+} complex were obtained (Fig. 4A). With the gradual increase of Hg^{2+} concentration, the band at 554 nm was gradually increased. When the concentration of Hg^{2+} was 5.0 eq., the absorbance (A_{554}) stabilized (Fig. 4B). In addition, the color of the solution changed from light yellow to pink upon addition of Hg^{2+}. For Hg^{2+} in a concentration range of 0–70 μM, the absorbance (A_{554}) displayed a great linear relationship ($Y = 0.0158X - 0.094$, $R = 0.983$). The UV/vis detection limit was calculated to be 0.679 μM based on $3\sigma/k$ (Fig. S8†).

Table 1 Comparative study of the analytical performance of **1** + Hg^{2+} with other recently reported probes

Structure	Media	Linear range	Detection limit	Approaches	Ref.
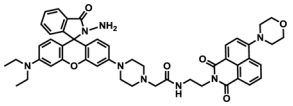	CH_3CN–H_2O (7/3, v/v)	0–21 μM	2.334 μM	Fluorescence	This work
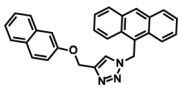	THF : H_2O (4 : 6)	—	1.25 μM	Fluorescence	7
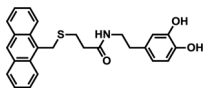	HEPES buffer	—	1.1 μM	Fluorescence	8
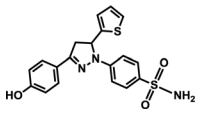	H_2O	20–200 μM	14.54 μM	Fluorescence	9
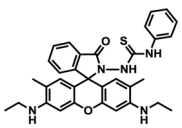	H_2O	0.9–12 μM	0.3 μM	Fluorescence	10

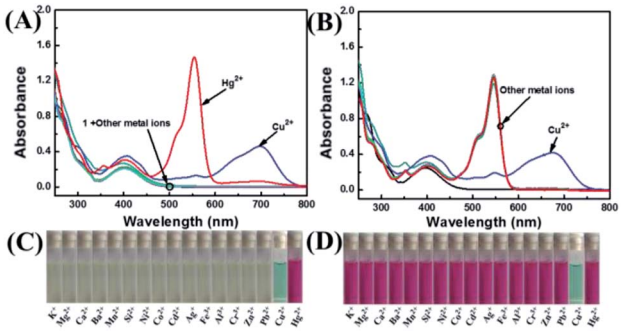

Fig. 3 Variations in the spectra of **1** induced by various metal ions: (A) absorption spectral alterations; (B) competitive tests for the absorption spectra of **1** upon addition of 5.0 eq. Hg^{2+} in the presence of 5.0 eq. other metal ions; (C) the photos of color variations; (D) the color pictures of **1** upon addition of 5.0 eq. Hg^{2+} in the existence of 5.0 eq. else metal ions.

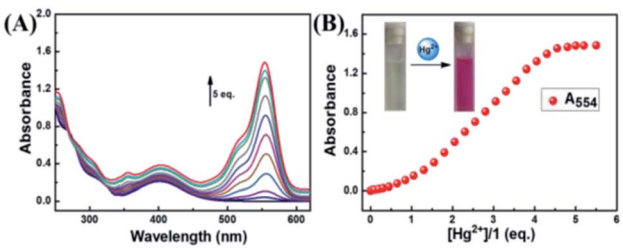

Fig. 4 (A) Absorption spectral changes of **1** in the presence of different amounts of Hg^{2+}; (B) the absorbance intensity at 554 nm.

Detection mechanism for Hg^{2+}

With the addition of Hg^{2+}, the probe showed orange fluorescence, which implied that the spirolactam ring of the rhodamine group was opened. In order to verify this process, ^1H NMR measurements were performed (Fig. 5A). In the spectrum of **1**, the peak (Ha) of spirolactam ring was located at 3.70 ppm. Upon the addition of Hg^{2+} to the solution of **1**, the peak disappeared because of the interaction between **1** and Hg^{2+}. To further confirm the interaction between **1** and Hg^{2+}, HPLC spectra of compound **7**, **1** and **1** + Hg^{2+} were recorded as shown in Fig. 5B. The retention time of **1** + Hg^{2+} was almost the same as that of compound **7**. In addition, ESI-MS measurements were performed with results shown in Fig. 5C. A characteristic peak at 835.2 *m*/*z* corresponding to $[\mathbf{M_1} + H^+]^+$ was obtained in the mass spectra and a familiar peak at 821.1 *m*/*z* appeared upon the addition of Hg^{2+}, which was the same as $[\mathbf{M_7}]^+$. Based on the above results, it was verified that probe **1** was hydrolyzed to rhodamine acid and the structure returned compound **7** (**1** + Hg^{2+} complex). A possible reaction mechanism[41] for Hg^{2+}-promoted hydrolysis was proposed as shown in Fig. 5D.

As illustrated in Scheme 2, the probe **1** was in the spirolactam ring-closing status and the FRET must remain closure before reacting with Hg^{2+}. The addition of Hg^{2+} caused the rhodamine acceptor to be in the ring-opening form through Hg^{2+}-promoted hydrolysis of rhodamine hydrazide to rhodamine acid as formerly reported,[42,43] and thus initiated the FRET process.

Cell culture and imaging

To investigate the membrane permeability of **1** in biological systems, HeLa cells (human cervical cancer cell) were incubated in DMEM (Dulbecco modified Eagle's medium) increasing 10% PBS in the condition of 5% CO_2 and 95% air at 37 °C. Subsequently, HeLa cells were cultured with compound **1** (20 μM) for 30 minutes and imaged with a fluorescent microscope. As

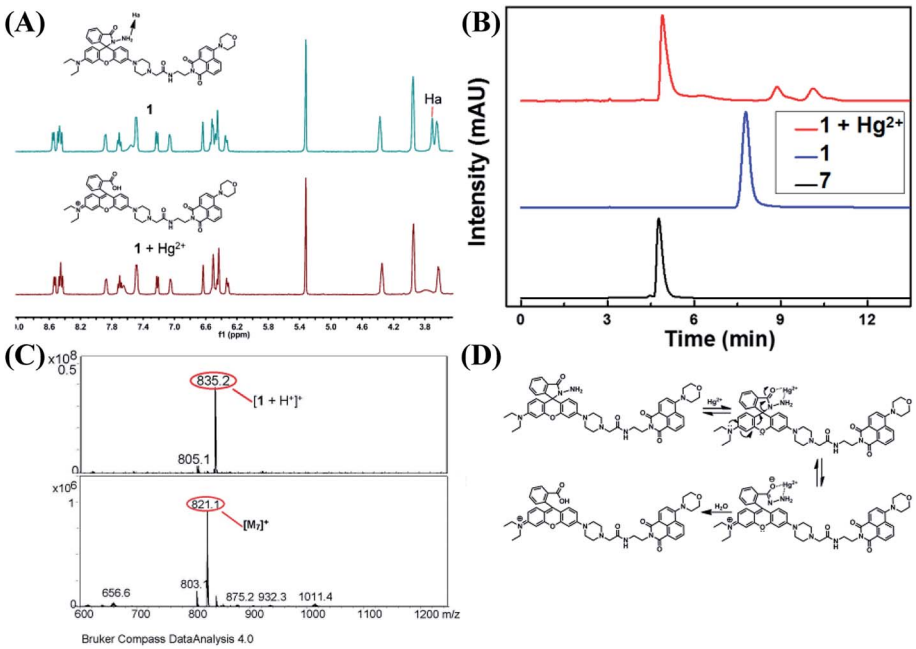

Fig. 5 (A) Partial ^{1}H NMR spectra of **1** and **1** upon addition of Hg^{2+} in CD_2Cl_2; (B) HPLC chromatograms of a mixture of **1** + Hg^{2+}, **1**, **7** (detected at 400 nm, with injection volume 50 μL, flow rate at 0.5 mL min^{-1} using CH_2Cl_2/C_2H_5OH (20 : 1, v/v) and room temperature); (C) ESI-MS spectra of **1** and **1** + Hg^{2+}; (D) a possible combination mode of **1** + Hg^{2+} complex.

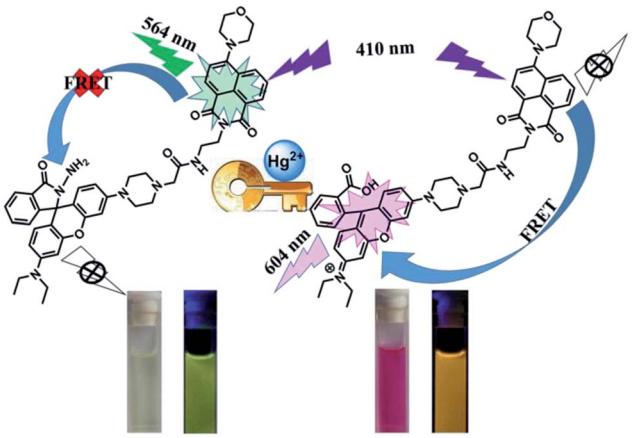

Scheme 2 The proposed mechanism of probe **1** for sensing Hg^{2+}.

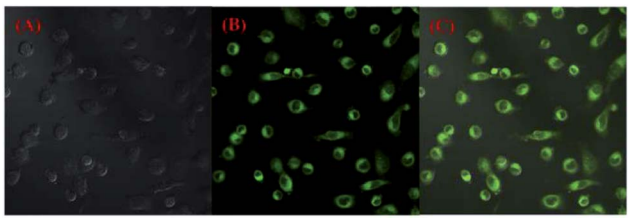

Fig. 6 Fluorescence images of HeLa cells with an excitation filter of 410 nm and emission collected at 500–700 nm: (A) bright field image; (B) dark field image; (C) merged images of (A) and (B).

illustrated in Fig. 6, a green fluorescence was observed. This result indicated that probe **1** was a promising candidate for cell imaging.

Conclusions

In conclusion, a rhodamine–naphthalimide probe has been developed. The Hg^{2+}-induced changes in color and fluorescence not only have high selectivity and sensitivity but also can be visualized by "naked-eyes". The probe also exhibited a good linear relationship in both fluorescence and UV-vis measurements. In addition, the spectral shifts of two obvious emission bands were up to 40 nm, which could reduce the interference of crosstalk signals, eliminate any influence of excitation backscattering, and improve the detection accuracy. Additionally, it was successfully applied to intracellular staining in biological applications. Therefore, the results reported here provided a novel approach for the recognition of Hg^{2+}.

Conflicts of interest

There are no conflicts of interest to declare.

Acknowledgements

The authors are grateful for the financial support from the National Natural Science Foundation of China (41867052, 21662015, 21861017, 41867053), the "5511" Science and Technology Innovation Talent Project of Jiangxi, the key project of Natural Foundation of Jiangxi Province (20171ACB20025), the Science Funds of Natural Science Foundation of Jiangxi Province (20171BAB203014, 20171BAB203011), the Masters' Innovative Foundation of Jiangxi Science and Technology Normal University (YC2018-X43).

Notes and references

1 X. Chen, T. Pradhan, F. Wang, J. S. Kim and J. Yoon, *Chem. Rev.*, 2011, **112**, 1910–1956.
2 Y. L. Fu, C. B. Fan, G. Liu and S. Z. Pu, *Sens. Actuators, B*, 2017, **239**, 295–303.
3 E. T. Feng, C. B. Fan, N. S. Wang, G. Liu and S. Z. Pu, *Dyes Pigm.*, 2018, **151**, 22–27.
4 Y. P. Xuan and J. B. Qu, *RSC Adv.*, 2018, **8**, 4125–4129.
5 X. L. Zheng, H. Li, W. Feng, H. C. Xia and Q. H. Song, *ACS Omega*, 2018, **3**, 11831–11837.
6 K. Y. Tan, C. Y. Li, Y. F. Li, J. J. Fei, B. Yang, Y. J. Fu and F. Li, *Anal. Chem.*, 2017, **89**, 1749–1756.
7 R. C. Gupta, S. S. Razi, R. Ali, S. K. Dwivedi, P. Srivastava, P. Singh, B. Koch, H. Mishra and A. Misra, *Sens. Actuators, B*, 2017, **251**, 729–738.
8 W. J. Feng, Q. X. Hai, Y. Zhou, Y. Ni, L. L. Wang, S. Jing, L. Li and W. Ji, *Talanta*, 2017, **167**, 681–687.
9 E. Bozkurt and H. I. Gul, *Sens. Actuators, B*, 2018, **255**, 814–825.
10 F. J. Orriach-Fernandez, A. Medina-Castillo, J. F. Fernandez-Sanchez, A. M. Pena and A. Fernandez-Gutierrez, *Anal. Methods*, 2013, **5**, 6642–6648.
11 A. Mohan and R. N. Kizhakayil, *ACS Appl. Mater. Interfaces*, 2016, **8**, 14125–14132.
12 S. H. Jing, C. H. Zheng, S. Z. Pu, C. B. Fan and G. Liu, *Dyes Pigm.*, 2014, **107**, 38–44.
13 D. Singhal, N. Gupta and A. K. Singh, *RSC Adv.*, 2015, **5**, 65731–65738.
14 Y. J. Gong, X. B. Zhang, Z. Chen, Y. Yuan, Z. Jin, L. Mei, J. Zhang, W. H. Tan, G. L. Shen and R. Q. Yu, *Analyst*, 2012, **137**, 932–938.
15 S. Gupta and M. D. Milton, *New J. Chem.*, 2018, **42**, 2838–2849.
16 Y. J. Gong, X. B. Zhang, C. C. Zhang, A. L. Luo, T. Fu, W. H. Tan, G. L. Shen and R. Q. Yu, *Anal. Chem.*, 2012, **84**, 10777–10784.
17 J. M. Hu, L. Dai and S. Y. Liu, *Macromolecules*, 2011, **44**, 4699–4710.
18 K. M. Vengaian, C. D. Britto, K. Sekar, G. Sivaraman and S. Singaravadivel, *RSC Adv.*, 2016, **6**, 7668–7673.
19 M. Kaur, Y. H. Ahn, K. H. Choi, M. J. Choa and D. H. Choi, *Org. Biomol. Chem.*, 2015, **13**, 7149–7153.
20 S. k. Yao, Y. Qian, Z. Q. Qi, C. G. Lu and Y. P. Cui, *New J. Chem.*, 2017, **41**, 13495–13503.
21 D. W. Huang, C. G. Niu, G. M. Zeng, X. Y. Wang and X. X. Lv, *Talanta*, 2015, **132**, 606–612.
22 P. Mahato, S. Saha, E. Suresh, R. D. Liddo, P. P. Parnigotto, M. T. Conconi, M. K. Kesharwani, B. Ganguly and A. Das, *Inorg. Chem.*, 2012, **51**, 1769–1777.
23 M. F. Czar, F. Zosel, I. König, D. Nettels, B. Wunderlich, B. Schuler, A. Zarrine-Afsar and R. A. Jockusch, *Anal. Chem.*, 2015, **87**, 7559–7565.
24 P. Siddhartha, S. Buddhadeb, M. Manjira, D. Koushik, Z. Ennio, K. M. Sushil, R. K. Anisur and C. Pabitra, *Analyst*, 2014, **139**, 1628–1631.
25 A. B. Othman, J. W. Lee, J. S. Wu, J. S. Kim, R. Abidi, P. Thuery, J. M. Strub, A. V. Dorsselaer and J. Vicens, *J. Org. Chem.*, 2007, **72**, 7634–7640.
26 Y. H. Lee, M. H. Lee, J. F. Zhang and J. S. Kim, *J. Org. Chem.*, 2010, **75**, 7159–7165.
27 C. Ma, F. Zeng, L. F. Huang and S. Z. Wu, *J. Phys. Chem. B*, 2011, **115**, 874–882.
28 X. L. Zhang, Y. Xiao and X. H. Qian, *Angew. Chem.*, 2008, **120**, 8145–8149.
29 J. F. Sun, B. Hua, Q. Li, J. Zhou and J. Yang, *Org. Lett.*, 2018, **20**, 365–368.
30 Y. X. Fu, H. Jin, X. N. Bu and R. J. Gui, *J. Agric. Food Chem.*, 2018, **66**, 9819–9827.
31 N. Melnychuk and A. S. Klymchenko, *J. Am. Chem. Soc.*, 2018, **140**, 10856–10865.
32 Y. Y. Wang, X. Xiang, R. Yan, Y. Liu and F. L. Jiang, *J. Phys. Chem. C*, 2018, **122**, 1148–1157.
33 J. M. Haimerl, I. Ghosh, B. König and J. M. Lupton, *J. Phys. Chem. B*, 2018, **122**, 10728–10735.
34 M. J. Liu, J. Yuan, J. Tao, Y. Q. Zhang, C. M. Liu and H. Z. Kou, *Inorg. Chem.*, 2018, **57**, 4061–4069.
35 J. Yuan, S. Q. Wu, M. J. Liu, O. Sato and H. Z. Kou, *J. Am. Chem. Soc.*, 2018, **140**, 9426–9433.
36 L. Liu and J. C. Dai, *Cryst. Growth Des.*, 2018, **18**, 4460–4469.
37 X. Zheng, R. Ji and X. Cao, *Anal. Chim. Acta*, 2017, **978**, 48–54.
38 J. C. Wu, T. Yi, T. M. Shu, M. X. Yu, Z. G. Zhou, M. Xu, Y. F. Zhou, H. J. Zhang, J. T. Han, F. Y. Li and C. H. Huang, *Angew. Chem., Int. Ed.*, 2008, **47**, 1063–1067.
39 L. He, X. Yang, Y. Liu and W. Lin, *Anal. Methods*, 2016, **8**, 8022–8027.
40 S. Wang, H. C. Ding, Y. S. Wang, C. B. Fan, Y. Y. Tu, G. Liu and S. Z. Pu, *RSC Adv.*, 2018, **8**, 33121–33128.
41 D. Virginie, F. Francis and W. Anthony, *J. Am. Chem. Soc.*, 1997, **119**, 7386–7387.
42 L. Song, X. D. Sun, Y. Ge, Y. H. Yao, J. Shen, W. B. Zhang and J. H Qian, *Chin. Chem. Lett.*, 2016, **27**, 1776–1780.
43 J. L. Tang, C. Y. Li, Y. F. Li, X. Lu and H. R. Qi, *Anal. Chim. Acta*, 2015, **888**, 155–161.